Real-time Electrode Misalignment Detection Device for RSW Basing on Magnetic Fields

D. Ibáñez[1] [a], E. García[2] [b], J. Martos[1] [c] and J. Soret[1] [d]

[1]*Dept. of Electrical and Electronic Engineering, University of Valencia, Burjassot, Valencia, Spain*
[2]*Ford Valencia, 46440, Valencia, Spain*

Keywords: Resistance Spot Welding, Detection, Hall Effect Sensors, Electrodes, Misalignment, Magnetic Field, Simulation.

Abstract: Electrodes misalignments are considered one of the most important mechanical factors involved in RSW (Resistance Spot Welding). Misalignment causes quality problems as undersized weld, expulsions or nonrounded-weld. Man-power needed in the automotive production lines is increased so as to repair the lack of quality, which means an increase in the cost of production. Consequently, an implantable solution for the automotive industry should be developed in order to detect misalignment when this happens. This research gives an answer by measuring the electrode misalignment by means of the generated magnetic field for the electrodes. The proposed method is validated by Multiphysics simulation measurement. Finally, this method is put into practice by creating a device tested in an automotive production line at the assembly and body plant in Ford Valencia. Together with the device, a communication system is implemented to carry out predictive management. This research initiates a novel line of research for the early and online detection of misalignment problems in welding guns.

1 INTRODUCTION

The resistance spot welding process bases its operation on a current flow from the tip of the upper electrode between the metals to be welded to the tip of the lower electrode. When the current circulates through the metals, and due to Joule's law, the heat generated melts the metals forming a weld joint between the metal sheets through the fusion and the result is a strong weld between sheets without additional substances. Therefore, the growth of the weld (welding nugget) depends on the density of welding current, the welding time, the force exerted by the electrodes on the sheets and the area of the electrode tip (Aravinthan et al., 2011)

This dependence is different depending on the parameter, since the time and the current make the welding, while the pressure and the area of the electrode tip have a direct relationship with the final quality of the welding.

Misalignment of the electrodes causes a variation in the contact area between the electrode tips. The alignment of electrodes can be classified into three types depending on their orientation. The electrodes can be perfectly aligned, axially misaligned or angularly misaligned, as shown in Figure 1 (Zhang et al., 2005).
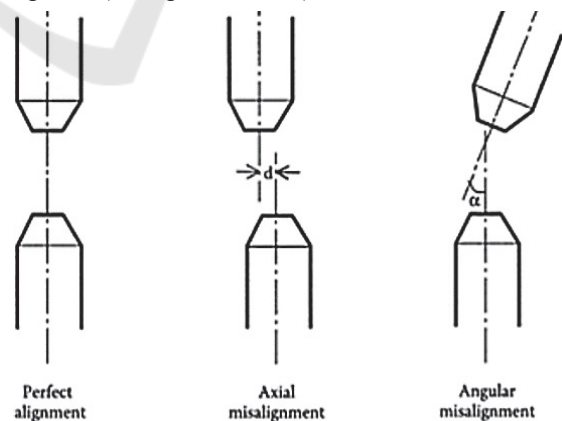

Figure 1: Types of electrode misalignment RSW.

[a] https://orcid.org/0000-0002-3917-9875
[b] https://orcid.org/0000-0002-4210-9835
[c] https://orcid.org/0000-0002-8455-6369
[d] https://orcid.org/0000-0001-8695-6334

Different studies have shown the alignment of the electrode plays an important role in the geometry of the welding point, Figure 2, in addition the misalignment of the electrode causes expulsion, which leads to poor welding zones Tang et al.,2003), (Charde,2012).

Figure 2: Poor-quality spot causes by misalignment.

Some authors have proposed different methods for detecting misalignment using image processing methods, by which they are able to determine the direction and angle of misalignment with good results (Li et al.2019). The main problem presented by this method is the cost of implementation for a high production line with many welding guns. Therefore, there is not a viable method for detecting misalignment in this type of production lines.

Due to the reasons mentioned above, there is a need to investigate a simple and economical method for the detection of misalignment, since what is sought is that it can be used in the high-production automotive industry.

The theoretical basis of this method is laid on the variation of the current density at the tip of the electrode. Specifically, what is intended with this method is to identify the change in current density as the misalignment appears.
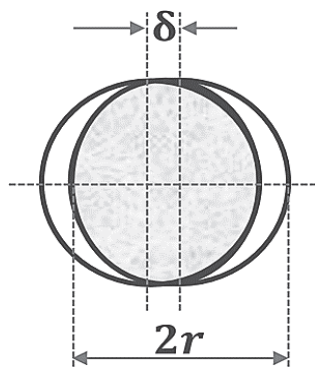

Figure 3: Geometric model for calculating contact area due to axial misalignment.

When the electrodes are misaligned, as shown in Figure 3, the contact area (Ca) of the electrode tips varies according to the equation 1.

$$C_a = 2r^2 \sin^{-1}\left(\sqrt{1 - \left(\frac{\delta}{2r}\right)^2} \right) - \delta \sqrt{r^2 - \left(\frac{\delta}{2}\right)^2}$$

where Ca is the contact area of the electrodes, r is the radius of the electrode and δ is the amount of misalignment.

It can be seen from the equation that the reduction of the contact area is strongly correlated with the axial misalignment.

From the Ampère's Integral Law can be obtained the relationship between the magnetic field (B) and the current density. This law relates the magnetic field intensity to its source, the current density.

$$\oint_C \vec{B} \cdot d\vec{l} = \mu_0 \int_S \vec{J} \cdot d\vec{S} + \mu_0 \varepsilon_0 \int_S \vec{E} \cdot d\vec{S}$$

Where the magnetic field is described by the variable B, the current density by J and the electric field by E.

Following the equation 2, it can be affirmed that if the current flows through the electrodes, and therefore there is a current density, a rotational magnetic field around the electrodes appear and the rotor of the magnetic field points in the same direction that the current density, this behaviour is represented in Figure 4.
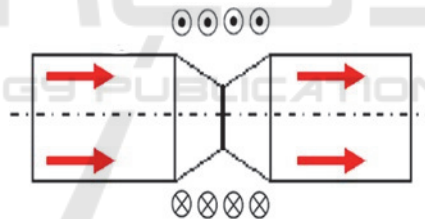

Figure 4: Generated Magnetic Field.

As a result, basing in this equation, it can be affirmed that when electrodes are misaligned, the contact area of the electrodes decreases, which produces a raising on the current density and consequently a magnetic field higher than which is generated with a correct electrode alignment.

2 MISALIGNMENT DETECTION METHOD

As shown in the previous section, a possible relationship between the magnetic field generated by the short-circuited electrodes and their misalignment can be deduced mathematically. The proposed method for the detection of the misalignment is

based on the measurement of the magnetic field in the contact plane of the electrodes.

The measurements should be carried out in such a way that a value is obtained for determining the direction of the misalignment of the electrodes.

For this, it is postulate that if the contact plane is divided into the Cartesian axes and measurements are made at different distances from the centre of the ideal contact surface of the electrodes, could be detected the misalignment of the electrodes and its direction.

This means that if the magnetic field can be measured in both Cartesian axes, both in positive and in negative, it will be possible to determine the difference of the magnetic field generated by the misaligned electrodes in comparison with the one generated by the perfectly aligned electrodes.

As it is a novel hypothesis, due to the fact that other researchers haven´t published anything related to the relationship between the magnetic field and the misalignment, it is fundamental to demonstrate it. Firstly, performing a validation by means of simulation of the physical phenomenon, to verify that, in fact, the mathematical assumption is fulfilled.

For the validation of this method, software of simulation of the physical phenomenon based on magnetic field theory is used.

Once the hypothesis has been validated for the proposed method, a device would be developed for taking measurements in an industrial environment, capable of determining the differences between simulation and real experimentation to finally design an automatic system for detecting problems of alignment of welding electrodes in real time.

3 MATERIALS AND METHODS

For the analysis of the behaviour of the magnetic field depending on the state of the misalignment, a physical phenomenon simulation software is drawn on. The simulations are carried out for the symmetry of an F- type electrode (ISO 5821, 2007) with the following data:

- Current flowing through the electrode: 8 kA.
- Diameter of the electrode tip: 6mm.
- Electrode body diameter: 20 mm.
- Cone height: 5mm.

These simulations are performed simulating a current flowing between the electrodes shorted. To obtain the relationship between misalignment and generated magnetic field.

During this validation, three tests will be performed. In the first one, the magnetic field

generated for an electrode in which $\delta = 0$ mm, i.e., a perfectly aligned electrodes, is simulated. In the second, the value of δ is increased up to 1mm and the magnetic field is simulated, comparing the values of both cases. Finally, the value δ is increased again up to 2mm and the simulation is carried out, comparing all the obtained values.

For each of the cases, two simulations are carried out. In the first simulation, the values of the magnetic field are collected depending on the distance on the x-axis to the centre of the electrode. These values are simulated for both the contact plane of the electrodes, $z = 0$ mm, as for planes situated $z = 10$mm and $z = -10$mm.

In the second simulation, the data is acquired in this case as a function of the displacement in the z-axis. In this simulation, two data curves are obtained: the variation of the magnetic field on the z-axis when $x = 20$mm and the variation of the magnetic field on the Z-axis when $x = -20$mm.

4 MAGNETIC FIELD SIMULATION

This section shows the results of the different simulations carried out as described in the previous section.

4.1 δ=0mm

As mentioned, simulations are carried out for three different scenarios. In this first case, two electrodes perfectly aligned are simulated, $\delta=0$ mm and S= 50.26 mm^2. This first case points what is the ideal value of the magnetic field generated by the electrodes. The following cases should therefore be compared with this to determine if there is certainly a relationship between the misalignment and the generated magnetic field.
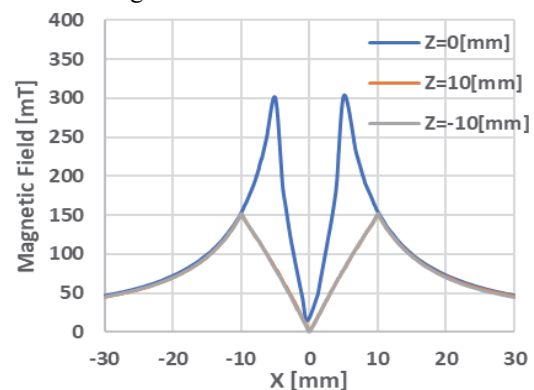

Figure 5: Magnetic Field Generated for aligned electrodes. X-axis displacement.

From this simulation, the data represented in Figure 5 and Figure 6 are obtained. As it can be seen, both in the data of Figure 5, which shows the evolution of the magnetic field on the x axis, and the one of Figure 6, which shows the evolution of the magnetic field in the y-axis, there is a symmetry in the generated magnetic field.

Hence, this means that when measuring at the same distances from the centre of the generated magnetic field, the same value is obtained. This point is very important because what is sought in this study is to be able to determine the misalignment but also the direction of it.

In addition, this data also shows how the Ampere law is fulfilled. By analysing the three curves of Figure 7, it can be observed how those taken on the planes z = -10mm and z = 10mm, present a lower magnetic field value. This is because at this height, the surface through which the intensity flows are S = 314.15mm^2. This makes the current density lower and therefore the magnetic field is lower too
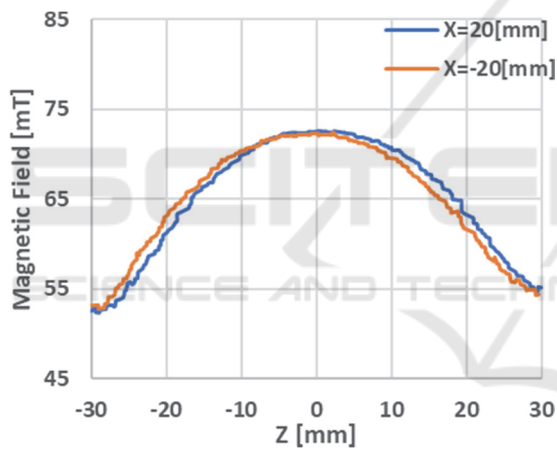

Figure 6: Magnetic Field Generated for aligned electrodes. z-Axis displacement.

4.2 δ=1mm

In this second case, electrodes with a displacement of the upper electrode of 1mm are simulated, that is, δ = 1mm. Using equation 1 it can be calculated that the contact surface for this case will be S = S·Cr = 50.26·0.7623= 38.31 mm^2.

Therefore, according to the hypothesis, the magnetic field generated by the electrodes must be higher since the current density increases.

Figure 7 shows how, as expected, the simulated magnetic field is greater than the magnetic field of Figure 5. The maximum value of the generated magnetic field is 340 mT, which represents an increase in the magnetic field by approximately 111%

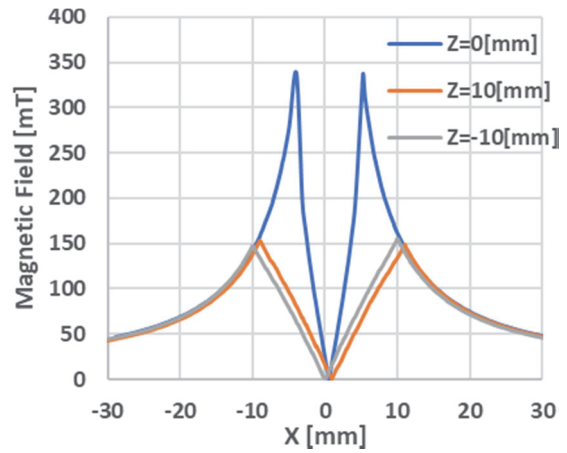compared to the field generated by the perfectly aligned electrodes.

Figure 7: Magnetic Field Generated for electrodes with δ=1mm.   X-axis displacement.

To make the comparison between the different cases, the data is analysed at 20mm from the centre of the magnetic field for the perfectly aligned electrodes. This centre is shown in the graphs as the zero of the coordinate axes. This analysis is done in a more graphical way observing the Figure 6 and 8 that represents the displacement in the Z-axis, since the data represented in it are those corresponding to the distances 20mm and -20mm.

If the data of x = 20mm and x = -20mm are taken at the time when z = 0mm, it can be observed that for the aligned electrodes this takes a similar value of 72 mT approximately.
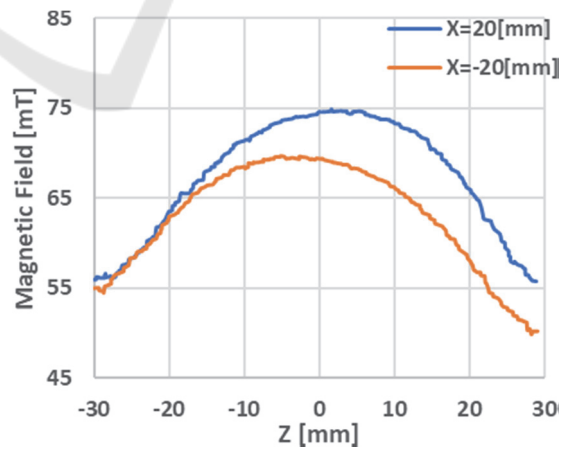

Figure 8: Magnetic Field Generated for electrodes with δ=1mm. z-Axis displacement.

On the other hand, with the data collected for this second case, it is observed that for x = 20mm the value of the magnetic field is equal to 74.5 mT, while

for x = -20mm the magnetic field is equal to 69,5mT. This means that while in the first case the difference between x = 20mm and x = -20mm is 0 mT, in the second case this difference increases significantly up to 5 mT.

It is also important to point out that because of the fact that one of the electrodes has moved but the other has been fixed, the centre of the magnetic field has been shifted 0.5 mm. This also rise the difference between the values in the x positive and negative x.

4.3 δ=3mm

In this last case the misalignment of the electrodes increases δ up to 3 mm. This supposes a misalignment of 50% of the maxim misalignment. This last simulation helps to determine in a more reliable way if it is possible to differentiate different states of misalignment.
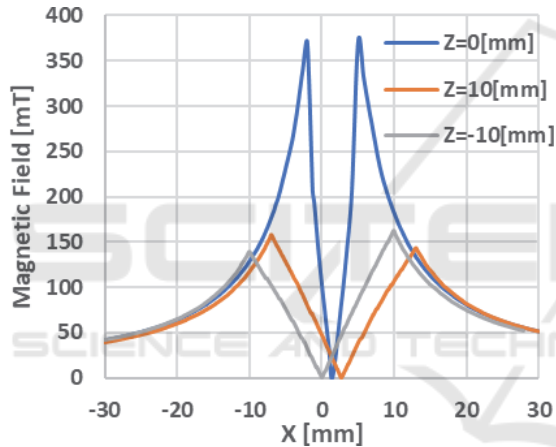

Figure 9: Magnetic Field Generated for electrodes with δ=2mm. X-axis displacement.

In this case, using equation 1 again, the actual contact surface of the electrodes can be calculated. Since δ has increased to 2mm, the ratio between the ideal surface and this new surface decreases to 0.5309. Therefore, the current surface is 26.68 mm^2.

As in the previous case, it can be seen in Figure 9 that the maximum magnetic field generated is higher than the other two cases, taking a value of 376 mT.

This represents an increase of 123% and 111% respectively.

Following in this case the previous analysis about the measurement differences between x = 20mm and x = -20 can be seen, as in the previous result, that there is no symmetry. For x = 20mm a value of 81 mT is recorded, while for x = -20mm a value of 65mT is recorded.
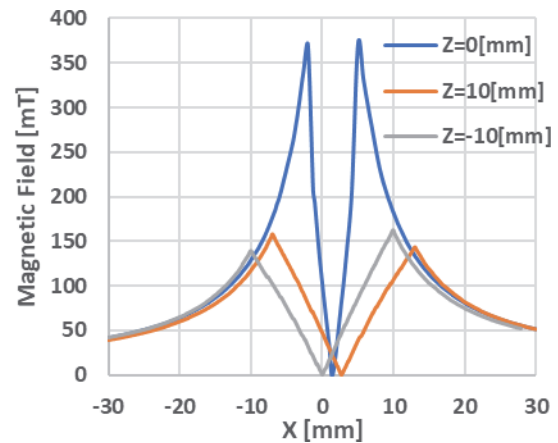

Figure 10: Magnetic Field Generated for electrodes with δ=2mm. X-axis displacement.

Therefore, in this third case it can be seen how the difference between both measures increases again while the misalignment increases too, going from a difference of 0 mT for the misaligned electrodes to a difference of 16 mT
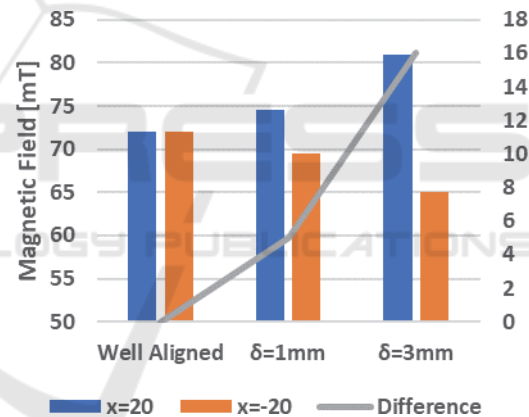

Figure 11: Summary of simulation result.

Finally, Figure 11 summarizes the most relevant values of this validation by simulation. Then, the results show that there is a strong relationship between the generated magnetic field and the alignment of the electrodes. So, the hypothesis has been validated.

5 SIMPLE DEVELOPMENT OF A DEVICE FOR THE DETECTION

Once the hypothesis has been validated, it is necessary to study how this new method can be applied to the high production industry of the automobile.

As it has been explained, it is necessary to make measurements of the magnetic field in the contact plane of the electrodes. Therefore, it is necessary to perform four measurements of the magnetic field, two for each of the axes x-y. For this, it is necessary to located sensors capable of performing these measurements at x = 20mm, x = -20mm, y = 20mm and y = -20mm.

In this case, two PCB are manufactured, one in which four low-cost hall effect sensors are located, which will be where the measurement is made. In this first PCB it is designed with a circular hole in the middle, so that the four hall effect sensors are distributed to perform measurements on the two cartesian axes.

In the second PCB the microcontroller used to control the signals collected by the sensors is located. To isolate the two PCBs, a 3D printed PCA encapsulation is performed. This design is made to optimize costs and increase the robustness of the design.

This device is designed so that the electrodes can be closed and positioned in the middle of the four sensors. Once located in that position, a current is passed between the short-circuited electrodes and the sensors measure the generated magnetic field.

Figure 12 shows the location on the real welding line of the PCB on which the Hall Effect sensors are mounted.

Figure 12: Actual PCB location for magnetic field measurement.

This measured magnetic field data is sent to the second PCB where the microprocessor that manages these signals is located. There the voltage values measured by the sensors are converted to magnetic field units.
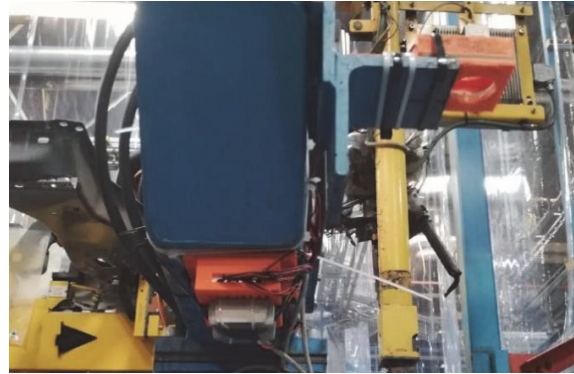

Figure 13: Actual PCB location for collection of the data.

Figure 13 shows the situation of the PCB, in which the microprocessor is located, in the actual welding line.

The signal management is carried out following the flow chart of Figure 15. Once the microcontroller is initialized, a first measurement of the magnetic field is made to determine the offset of the sensors, thus eliminating the possible differences between the measurements.
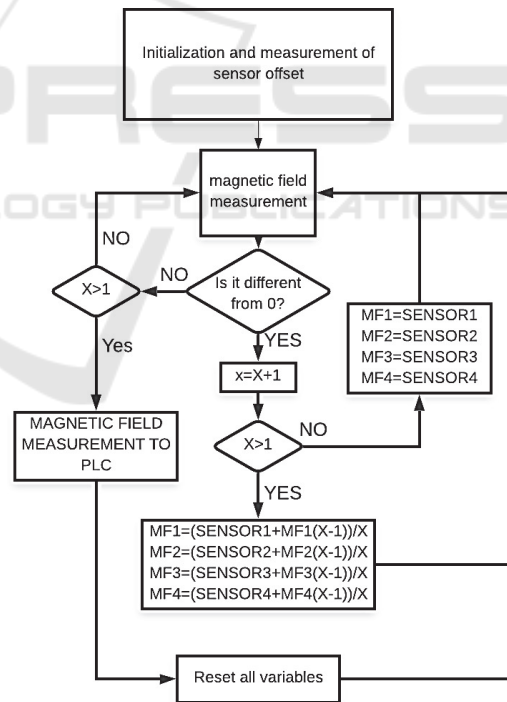

Figure 14: Operating flow chart.

Once this action is carried out, the four sensors begin to record the magnetic field value, if the measured magnetic field is zero, the microcontroller does not perform any calculation. Once the electrodes are short-circuited and generate a magnetic field, the
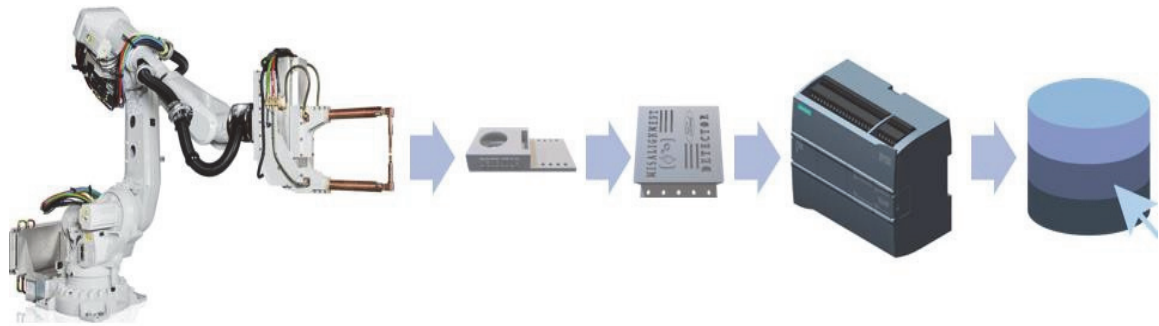
Figure 15: Measurement process flow.

microcontroller begins to register the values by calculating at all times the average value of the magnetic field measured in that period of time, so that the possible peaks that could appear are reduced by Use the average.

When the electrodes stop conducting current, the sensors re-measure the absence of magnetic field and at that time, the microcontroller sends the values to the PLC.

After communication with the PLC, the variables are reset to 0 and the measurement is restarted waiting again for the magnetic field generated by the electrodes in short circuit.

6 REAL-TIME CONTROL APPLICATION

Once a device capable of detecting the magnetic field has been developed, and therefore, the problems of alignment of the electrodes in the welding clamps, it is necessary to develop a final system capable of carrying out preventive maintenance on the actual welding line.

In such a way that patterns of misalignment behaviour and work limits are established based on history and experimentation. To do this, once the process described in Figure 14 is finished, when the data is already in the PLC, this data is stored in a database and sent to a web server. This whole process can be summarized in Figure 15.

In this case, in order to reduce the number of variables on which to perform the analysis, the four variables of each of the sensors are reduced by only two.

These two variables are calculated by subtraction between the sensors placed antiparallel, therefore, the two final variables will represent the displacement of the centre of the magnetic field on the X and Y axes, eliminating the absolute value of each of the four sensors.

Starting from the established values of the simulation first and after the values stored in the history, the alarm and pre-alarm levels for each of the Cartesian axes can be established. As shown in figure 16.
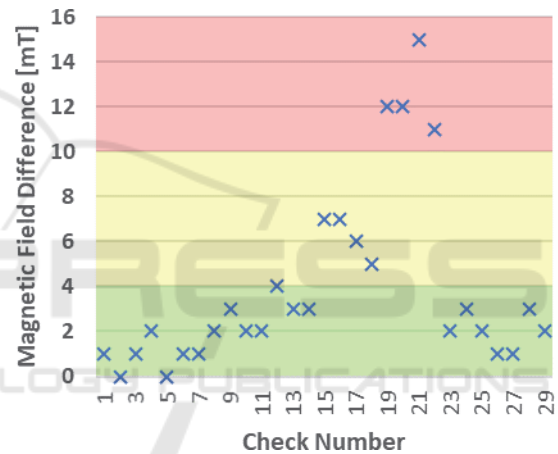

Figure 16: Example of alarms based on simulation.

Currently, this whole real-time medicine process is installed in a welding line. This application allows to obtain the data of each check in the attempt in which it is performed.

This last part of the investigation is still in an exact process of validation, since it is convenient to test all the cases and the real behaviour of a welding clamp, beyond the simulation results.

7 CONCLUSION

This article tries to give a solution to this important problem of misalignment in the electrodes of the welding guns. This problem directly affects the costs of production of automobile manufacturing, so it is mandatory to find a solution that can be implantable, i.e., a solution that does not involve a high cost of implementation. This article responds positively,

presenting a method for detecting the misalignment by magnetic fields.

For the method validation, mathematical calculations and simulations are used, in which it is observed how, unequivocally, there is a strong relationship between both factors.

Finally, a device for measuring the magnetic field is proposed, this device is composed of four hall effect sensors managed by a microcontroller. For the validation of the sensor, tests in a line of production of the automobile in Valencia Body and Assembly plant are carried out.

Although the data collection is not yet extensive enough, a historical data collection is begun to monitor the behaviour of the magnetic field generated by real misaligned electrodes.

In future investigations, the data obtained in the actual welding line should be analysed. Based on these results, a possible update of the method and the designed device should be performed.

In addition, an exhaustive study of the influence of the existing noises on the production lines and their influence on the measures taken must be made.

ACKNOWLEDGEMENT

REFERENCES

Aravinthan, A. and Nachimani, C. 2011. Analysis of Spot Weld Growth on Mild and Stainless Steel. *Welding Journal August 2011: 143-147.*

Claude Cohen-Tannoudji; Bernard Diu et Frank Laloë 1977. *Mécanique Quantique, vol. I et II. Paris: Collection Enseignement des sciences (Hermann).*

Richard Feynman 1974. Feynman lectures on physics Volume 2. *Addison Wesley Longman.*

ISO 5821 [2007] Resistance Spot Welding Electrode Caps.

Tang, He (Herman) & Hou, W. & Hu, S.J. & Zhang, H.Y.& Feng, Z. & Kimchi, Menachem. 2003. Influence of welding machine mechanical characteristics on the resistance spot welding process and weld quality. *Welding Journal. 82. 116/S-124/S.*

Charde, Nachi Mani. 2012. Effects of electrode deformation on carbon steel Weld. *International Journal of Advance Innovation, Thoughts and Ideas. 1. 8.*

Li, Yanqing & Tang, Guokun & Ma, Yongsheng & Shuangyu, Liu & Ren, Tao. (2019). An electrode misalignment inspection system for resistance spot welding based on image processing technology. *Measurement Science and Technology. 30.* 10.1088/1361- 6501/ab1245.

Zhang, H. & Senkara, J. 2005. Resistance welding: Fundamentals and applications.

Walker, Jearl; Halliday, David; Resnick, Robert 2014. Fundamentals of physics (10th ed.). *Hoboken, NJ: Wiley. p. 749.*